13 October 2000

ELSEVIER

Chemical Physics Letters 329 (2000) 42–46

CHEMICAL PHYSICS LETTERS

www.elsevier.nl/locate/cplett

Measurement of quenching rates of CO($a^3\Pi, v = 0$) using laser pump-and-probe technique

Ingrid J. Wysong *

Air Force Research Laboratory, AFRL/PRSA, 10 E. Saturn Blvd., Edwards AFB, CA 93524, USA

Received 17 April 2000; received in final form 30 June 2000

Abstract

Measurements are presented of rates of electronic quenching of CO(a, $v = 0$) by several gases. A pump-and-probe technique is used; CO(a) is created by pumping the spin-forbidden (a–X) transition at 206 nm. Measured rate coefficients at room temperature are $k_Q(CO) = 5.7 \pm 1.2$, $k_Q(NO) = 17 \pm 6$, $k_Q(N_2) = 1.4 \pm 0.6$, $k_Q(O_2) = 6 \pm 2$, $k_Q(H_2) = 2.6 \pm 1.0$, $k_Q(H_2O) = 33 \pm 12$ in units of 10^{-11} cm^3 s^{-1}.

1. Introduction

Cameron band emission, CO($a^3\Pi$–$X^1\Sigma$), is of interest as a source of ultraviolet (UV) radiation in flames [1] and in high-altitude rocket plumes [2,3]. In addition, it has been observed in the atmosphere of Mars [4] and in comets [5]. Due to its long radiative lifetime, the majority of the CO(a) molecules that exist in a flame or an atmosphere are lost to collisional quenching, even at fairly low gas densities. Thus, the estimated amount of Cameron band emission is extremely sensitive to the value of the quenching rate coefficient.

The CO(a) state is the lowest electronically excited state of the CO molecule, but the transition to the ground state is spin forbidden. Therefore, this state is metastable, with a natural lifetime of 3.7 ms [6]. Because it is metastable, the CO(a) state's quenching rate is very difficult to measure. This difficulty has led to a large scatter in the various literature values for quenching by most common gases. In addition, no value has been reported for quenching due to water, which is an important collider species in many environments.

2. Experimental approach

Laser pumping of the weak CO(a–X) intercombination transition has been previously demonstrated [7–10]. Laser-induced fluorescence (LIF) detection of CO(a) produced in a glow discharge has been demonstrated by Clyne and Heaven [11]. Here, a laser pump-and-probe approach, similar to a previous double resonance study [9] of CO($b^3\Sigma^+$) is used. A pulsed (6 ns pulse width), tunable laser at 206 nm promotes a small number of CO(X, $v = 0$) molecules to the (a, $v = 0$) state via the very weak (a–X) intercombination transition. After the pump laser populates a single rotational level in the (a, $v = 0$) state, rapid rotational redistribution occurs over approximately 10 ns due to collisions with the gases in the cell, creating a thermal rotational distribution. This step causes the major

* Corresponding author. Fax: +1-661-275-6245.
E-mail address: ingrid.wysong@ple.af.mil (I.J. Wysong).

0009-2614/00/$ - see front matter
PII: S0009-2614(00)00967-2

difficulty with the experiment, since the small CO(a) population is spread over a large number of quantum levels (three spin–orbit states and all the thermally populated rotational levels), only one of which is probed by the LIF detection, yielding a small signal. A Coherent 699-29 cw ring dye laser is used to continuously probe the population of the CO(a) state via LIF. The probe laser operates at 602 nm and excites the strong 'triplet system' ($d^3\Delta$–$a^3\Pi$) electronic transition on the (4,0) vibrational band. Subsequent fluorescence in the (4,2) band at 760 nm is detected to monitor the variation of CO(a) population as a function of time after the pump laser pulse. While it is known that the CO(d) state will easily collisionally transfer population to other nearby electronic states [12], the effect of this process should be indistinguishable in the present experiment from other types of collisional quenching of the CO(d) state. The mixing of the excited triplet states will result in reduced LIF signal but should not affect the time-dependence, which is due only to the decrease of the CO(a) population.

LIF detection has an advantage over trying to detect CO(a–X) emission directly in that it can be accomplished on a μs timescale, which greatly reduces the effects of diffusion or wall losses that are important on the millisecond timescale. On the other hand, LIF probes only one of the many quantum levels that are populated within the CO(a, $v = 0$) state. Also, it is susceptible to reduction in efficiency due to quenching of the CO(d) state. In fact, data on quenching of CO(a) by CO_2 could not be obtained in the present experiment, as addition of even very small amounts of CO_2 strongly quenched the CO(d–a) emission, thus making the LIF detection too insensitive.

To initially find the correct pump laser wavelength with no LIF probe, much higher CO pressures are used, along with a tighter UV focus and a biased wire pair in the cell to collect resonance-enhanced multi-photon ionization (REMPI) signal. The REMPI signal is very noisy but is adequate to tune the pump laser to the center of a (relatively) strong bandhead line of the (a–X) transition. The probe laser wavelength is set near a resonance line using a wavemeter and tuned manually to the peak by observing the LIF signal. After setting the probe laser wavelength on the peak of one of the strong CO(d–a) lines, the laser's locking feature is used to insure stability.

The experimental cell is a simple cube with a large window on one side to collect LIF and apertured Brewster's angle windows for laser beams to come in and out. The UV and visible beams are counter-propagating along the cell axis. The UV beam is softly focussed in center to about 1 mm diameter. It was found that a tighter focus, while convenient for adjusting the UV pump laser wavelength to the appropriate peak value with REMPI detection, produced a detectable background signal during the probe laser measurements due to the UV laser only (it is presumed that this background signal occurs due to recombination of the laser-created ions into excited electronic states that then emit fluorescence). The visible beam diameter is 3 mm, which insures that during the μs measurement time in 4 Torr of helium buffer gas, CO(a) molecules created in the center by the UV beam do not diffuse out. Good centering of the UV beam inside the visible beam is checked before each run by removing a side flange.

Ultra-high purity gases pass through individual mass flow meters and are mixed well before the interaction volume. The procedure, mentioned in some of the previous quenching measurements (discussed below), of diluting the collider gas in a buffer prior to measuring the flow rate was not considered necessary here. A small mechanical pump maintains a slow flow (less than 200 cm/s) through the cell. The cell pressure was in the range 5–7 Torr. Partial pressures of the various gases are calculated from the ratio of the partial mass flow to total flow rate times the cell pressure (measured with a 100 Torr capacitance manometer). Flow meters were calibrated using a wet test meter. As other collider gases were added, the CO flow was also increased slightly in order to maintain a constant partial pressure of CO as the partial pressure of collider gas was varied.

For the water measurement, a second helium flow was passed through a bubbler (after the mass flow meter) of distilled water with a separate pressure meter before a needle valve and then combined with the buffer helium and CO. The mass flow rate of water is given by

$f(\mathrm{He}) \times \mathrm{SVP}/(P - \mathrm{SVP})$, where SVP is the saturated vapor pressure of H_2O at the measured temperature, P the pressure in the bubbler, and $f(\mathrm{He})$ is the mass flow of He through the bubbler. The flow through the bubbler into the cell is maintained for sometime before data are acquired so that initial saturation of H_2O to the tubing and cell walls is completed.

LIF is collected and focused onto a small aperture using two lenses. A color glass filter (RG715) and a 760 nm bandpass filter are used to eliminate other light and a red-sensitive PMT detects the LIF. The PMT signal is fed directly into a digital oscilloscope where many laser shots (typically 500 for a given decay rate measurement) are averaged and the time-dependent signal is stored for further analysis. A background signal with the probe laser blocked, which shows a 20 ns spike, is taken; the LIF time scan is fitted starting from the end of the background spike.

The time variation is fitted to an exponential function to give a single value of decay rate for a given condition of gas pressure and composition. As can be seen in Figs. 1 and 2, however, the signal-to-noise ratio is rather poor, which leads to large uncertainties in the decay rate obtained from each fit. Fig. 3 provides an illustration of this uncertainty. Each time decay for the N_2 data set is fit to an exponential starting at the end of the background spike ($t = 0.02$ μs) where the signal is about 70–80% of its peak value and ending when the signal reaches 20% of its peak value. Then, each decay is fit a second time, starting at the same point, but extending to the point where the signal has reached 5% of its peak value. The two results are displayed as the upper and lower values of the error bars in the figure, with the data point in the middle (indicated by the filled circle) assumed to be the average of the two results. As can be seen, in some cases the two different fits give almost the same result for decay rate, while in others they vary considerably. This leads to the large quoted uncertainties in the final rate coefficients.

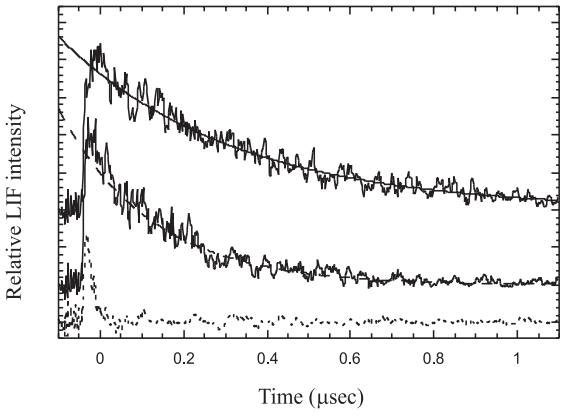

Fig. 1. Sample LIF data showing decay in CO(a) population after pump pulse. Top scan is with 1.2 Torr of CO; Middle scan is with 1.2 Torr of CO and 0.38 Torr of NO; bottom scan shows the background signal (probe laser blocked). The three have offset baselines for clarity. Exponential fits are indicated.

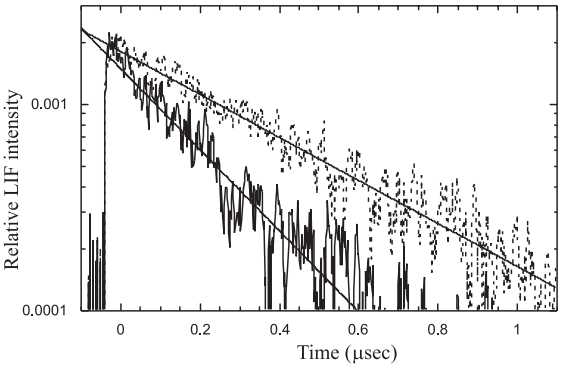

Fig. 2. Same sample data as Fig. 1, semi-log scale. The fit for the upper scan has a characteristic decay rate of 2.4 μs^{-1}, the lower scan fit has a rate of 4.8 μs^{-1}.

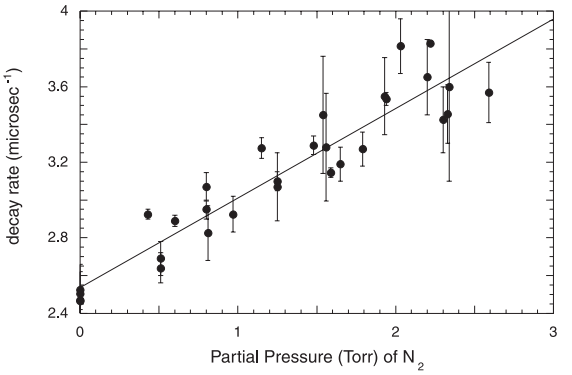

Fig. 3. Pressure dependence of decay rate for N_2 collider (plus 1.2 Torr CO, plus 4 Torr helium buffer gas). See text for explanation of error bars.

Fig. 4 shows the results for CO, O_2, and H_2 colliders, and Fig. 5 shows the results for NO and H_2O colliders. The variation in decay rate with partial pressure of a particular collider gas species (i.e., the slope in Figs. 3–5) yields the quenching rate coefficient, k_Q, for that species. Each set of points for decay rate versus collider pressure is the combination of data obtained on two or three different days. The intercept is expected to be zero for the CO collider case (Fig. 4) and equal to the decay rate due to 1.2 Torr of CO for the other colliders. Water vapor is shown to be an extremely efficient quencher. The other gases measured, however, typically produce a smaller value of k_Q than previously reported in the literature.

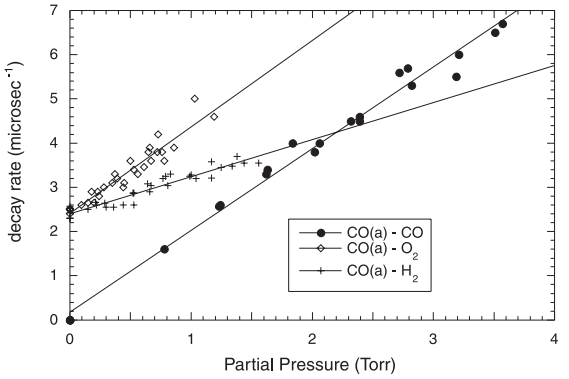

Fig. 4. Pressure dependence of decay rate for CO, O_2, and H_2 collider (plus 4 Torr helium buffer gas).

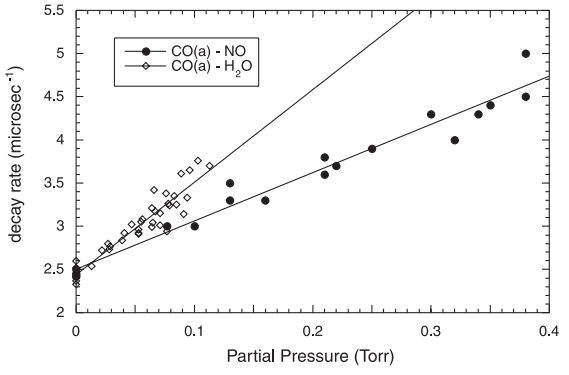

Fig. 5. Pressure dependence of decay rate for H_2O and NO colliders (plus 1.2 Torr CO, plus 4 Torr helium buffer gas).

3. Results

The measured values, as shown in Table 1, tend to be lower than those previously reported in the literature. One possible source of error in the present measurements, the presence of impurities (such as water) in the collider gas flows, would lead to an apparent increase in k_Q. No mechanism is known that would cause the measured values to be anomalously low. Any impurities in the helium buffer gas would only change the intercept, not the slope, of the decay rate-versus-pressure plots, and are not believed to be significant here. It may be noted that the previous measurements have been performed in flowing afterglows where the method of production of CO(a) is not as clean as used here. However, there is not any known flaw in the previous results. The major difficulty with the present method is that the signal-to-noise ratio is quite low. No value for quenching due to water has been previously reported and, as expected, water is a very efficient quencher.

Taylor and Setser [13] state that their results for k_Q should be lower limits, but probably within a factor of two of the true value, with relative values good to within 20%. Slanger and Black [14] quote a 10% uncertainty in their values for k_Q and Young and co-workers [15–17] quote 25%. The rate coefficient for N_2 quenching reported by Young and Morrow [17] is dependent on the value for CO quenching used in the analysis. If the present CO value (about one-half the value used by Young) were used in the analysis, the resulting value for N_2 would be decreased by 2, causing it to be even smaller in comparison to other measurements (including the present one). It may be noted that a very recent measurement of k_Q with CO_2 collider [18] yields $k_Q = (1.0 \pm 0.2) \times 10^{-11}$ cm^3/s , which is lower than most of the previous values for CO_2: 2.0 [13], 4.8 [19], 1.7 [14], and 1.2 [20].

As a check, data on NO self-quenching using LIF of NO(A, $v = 2$) fluorescence (which can be pumped by UV light near 206 nm) were obtained in the same cell and yielded a value of $(1.95 \pm 0.04) \times 10^{-10}$ cm^3/s, which compares very reasonably to the literature values of 1.75, 1.55, and 1.97 (Refs. [21–23], respectively).

Table 1
Measured quenching rate coefficients for CO(a, $v = 0$) (10^{-11} cm^3/s)

Collider gas	Present work (295 K)	Taylor and Setser [13] (300 K)	Wauchop and Broida [19] (300 K)	Slanger and Black [14] (300 K)	Young and co-workers [15–17]
CO	5.7 ± 1.2	11		7.6	12 ± 3
NO	17 ± 6	18	32 ± 16	23	31 ± 8
N_2	1.4 ± 0.6	0.9	3.8 ± 1.8		0.1
O_2	6.0 ± 2.0	20		14	12
H_2	2.6 ± 1.0	20		16	
H_2O	33 ± 12				

It is always interesting to consider the possible energy transfer pathways that may affect these quenching rate coefficients, but unfortunately, no data have been obtained in the present study that add to the knowledge of these pathways. It is noted that CO(a, $v = 0$) has no electronic state that is near or lower in energy, other than the ground state, so it is presumed that removal of CO(a) must lead either to CO(X, high v) or to a large amount of energy being absorbed by the collider. In the case of CO collider, the reaction to $C + CO_2$ may play a role. The detailed mechanism for the energy transfer in the quenching processes measured here is not known. It is known [14] that quenching of CO(a) by NO produces NO(A, B); the available pathway to nearby vibronic levels probably enhances the quenching process. For N_2 collider, CO(a, $v = 0$) does not have quite enough energy to produce N_2(A), which may explain its lower rate coefficient, but this path certainly contributes to the increasing rate that has been observed [13] for quenching of higher CO(a, v) states by N_2. As pointed out by Slanger and Black [14], CO(a) contains sufficient energy to dissociate O_2 or H_2, but no evidence has thus far been obtained that this process does occur. Further studies which probe the post-collision species would be desirable.

Acknowledgements

Support for this work was provided by the Air Force Office of Scientific Research under Dr. Mitat Birkan. The author would like to thank Dr. Larry Bernstein of Spectral Sciences for generously providing computed Franck–Condon factors and the reviewer for valuable comments.

References

[1] M.L. Burke, W.L. Dimpfl, P.M. Sheaffer, P.F. Zittel, L.S. Bernstein, J. Phys. Chem. 100 (1996) 138.
[2] G.V. Candler, D.A. Levin, R.J. Collins, P.W. Erdman, E. Zipf, C. Howlett, J. Thermophys. Heat Transfer 7 (1993) 709.
[3] D.A. Levin, G.V. Candler, R.J. Collins, AIAA J 35 (1997) 288.
[4] J.L. Fox, Can. J. Phys. 64 (1986) 1631.
[5] H.A. Weaver, P.D. Feldman, J.B. McPhate, M.F. A'Hearn, C. Arpigny, T.E. Smith, Astrophys. J. 422 (1994) 374.
[6] R.T. Jongma, G. Berden, G. Meijer, J. Chem. Phys. 107 (1997) 7034.
[7] M. Drabbels, S. Stolte, G. Meijer, Chem. Phys. Lett. 200 (1992) 108.
[8] J.M. Price, A. Ludviksson, M. Nooney, M. Xu, R.M. Martin, A.M. Wodtke, J. Chem. Phys. 96 (1992) 1854.
[9] R.T. Jongma, M.G.H. Boogaarts, G. Meijer, J. Mol. Spectrosc. 165 (1994) 303.
[10] S. Harich, A.M. Wodtke, J. Chem. Phys. 107 (1997) 5983.
[11] M.A.A. Clyne, M.C. Heaven, J. Chem. Soc. Faraday Trans. 77 (1981) 1375.
[12] T.G. Slanger, in: A. Fontijn, M.A.A. Clyne (Eds.), Reactions of small transient species, Academic Press, London, 1983, pp. 231.
[13] G.W. Taylor, D.W. Setser, J. Chem. Phys. 58 (1973) 4840.
[14] T.G. Slanger, G. Black, J. Chem. Phys. 55 (1971) 2164.
[15] R.A. Young, G. van Volkenburgh, J. Chem. Phys. 55 (1971) 2990.
[16] W. Felder, W. Morrow, R.A. Young, Chem. Phys. Lett. 15 (1972) 100.
[17] R.A. Young, W. Morrow, J. Chem. Phys. 62 (1975) 1994.
[18] M.P. Skrzypkowski, T. Gougousi, R. Johnsen, M.F. Golde, J. Chem. Phys. 108 (1998) 8400.
[19] T.S. Wauchop, H.P. Broida, J. Chem. Phys. 56 (1972) 330.
[20] G.M. Lawrence, Chem. Phys. Lett. 9 (1971) 575.
[21] T. Imajo, K. Shibuya, K. Obi, I. Tanaka, J. Phys. Chem. 90 (1986) 6006.
[22] H. Zacharias, J.B. Halpern, K.H. Welge, Chem. Phys. Lett. 43 (1976) 41.
[23] M. Asscher, Y. Haas, J. Chem. Phys. 76 (1982) 2115.